Average Heat Flux Characteristics of a Compact Rotating Detonation Engine for Space Propulsion

John Z. Ma, Yuechen Hou, Yingnan Wang, Xiangjun Zhang, Xiaojian He, Jian-Ping Wang
Center for Combustion and Propulsion, CAPT & SKLTCS
Dept. of Mechanics and Engineering Science, College of Engineering, Peking University
Beijing 100871, People's Republic of China

1 Introduction

Rotating detonation engine (RDE) is a new concept jet engine that is expected to bring a technical revolution to current aviation and aerospace propulsion systems. The RDE has practical value due to its intrinsic advantages, including one-time initiation, continuous mode operation, step increase in efficiency, self-sustaining and self-compression of detonation waves, large effective thrust at a low-pressure ratio, a wide range of inflow velocity, and design simplicity [1].

The basic concept of continuous detonation waves was proposed and conducted by Nicholls [2] and Voitsekhovskii [3]. For engineering applications, thermal management of RDEs has become a key technology that urgently needs breakthroughs, especially in the past three years, full-scale and long-duration prototype tests based on liquid fuels have been implemented. Due to the high-frequency RDWs, the combustor is subjected to an extremely complex and changeable heat flux environment. Meyer et al. [4, 5] studied characterization of heat transfer coefficientsand parameter impact on heat fluxin RDEs. It was shown that the heat transfer coefficient had a higher bulk value at the higher axial location and increasing the equivalence ratio (0.6 - 1.2) resulted in the bulk heat flux increasing. Kublik et al. [6] analyzed heat loads that occur in the region of detonation propagation in pulse and rotating detonation engines. Lim et al. [7] also studied the wall heat flux in a rotating detonation rocket engine, and it was shown that the heat fluxes in the detonation wave region appeared to be relatively higher than in the product region downstream of the detonation waves. Goto et al. [8, 9]evaluated the heating environment of RDE with different nozzles and propellant cooling. It revealed that the heat flux was roughly proportional to channel mass flux and the increase in the wall heat flux was only 18 - 25% with propellant injection cooling even when the flow rate was doubled.

However, there are few studies on the wall heat flux distribution and influencing factors of the whole rotating detonation combustor (RDC). In this paper, a compact RDE was designed, and a series of effective experimental tests for high-frequency heat flux measurement were carried out. The characteristics of instantaneous heat flux and the spatial distribution of the average heat flux were analyzed, and the effects of mass flow rate and equivalent ratio were discussed.

Correspondence to: mazhuang@pku.edu.cn

2 Experimental Setup and Methodology

The experimental data presented was collected at the Combustion and Propulsion Laboratorys Detonation Engine Research Facility at Peking University. The investigation was conducted on a RDE test section at flow rates from 60 to 160 g/s, and equivalence ratios from 0.3 to 1.8, using methane/GOX. An optimized hole-slot intake mode of the injector was adopted in the combustor. The experimental device, sensor arrangement and schematic diagram of RDC are shown in Figure 1. The length of the combustion chamber is L=69 mm, the inner radius R1=23 mm, the outer radius R2=29 mm, and the throat radius R3=26 mm. The net weight of the engine is 5 kg, which is expected to be further optimized to reduce to less than 3 kg. The design thrust is 500 N and the design chamber pressure is 1 Mpa.

Three PCB sensors are used to capture the high-frequency pressure curve of the detonation wave.The injection pressure and combustor pressure was captured by five static pressure sensors. In particular, 12 high-frequency coaxial E-type thermocouples were mounted flush on the wall of the combustor in order to obtain the transient wall heat flux. The response time of the coaxial thermocouple is less than 5 μs. The measurement range of heat flux was 0-50 MW/m^2, and the measurement error is less 7%.

A high-speed camera was used to image the natural flame from the aft end of the RDE. Images were recorded at a rate of 50000 frames per second, with an exposure time of 5.0 μs. The high-speed images allow for an assessment of the number, direction, and location of the waves in the annulus. Operation is computer-controlled and monitored by a 500 kHz data acquisition system. The stable working stage of the engine is selected as the criterion for data processing, as shown in Fig. 2 (left).

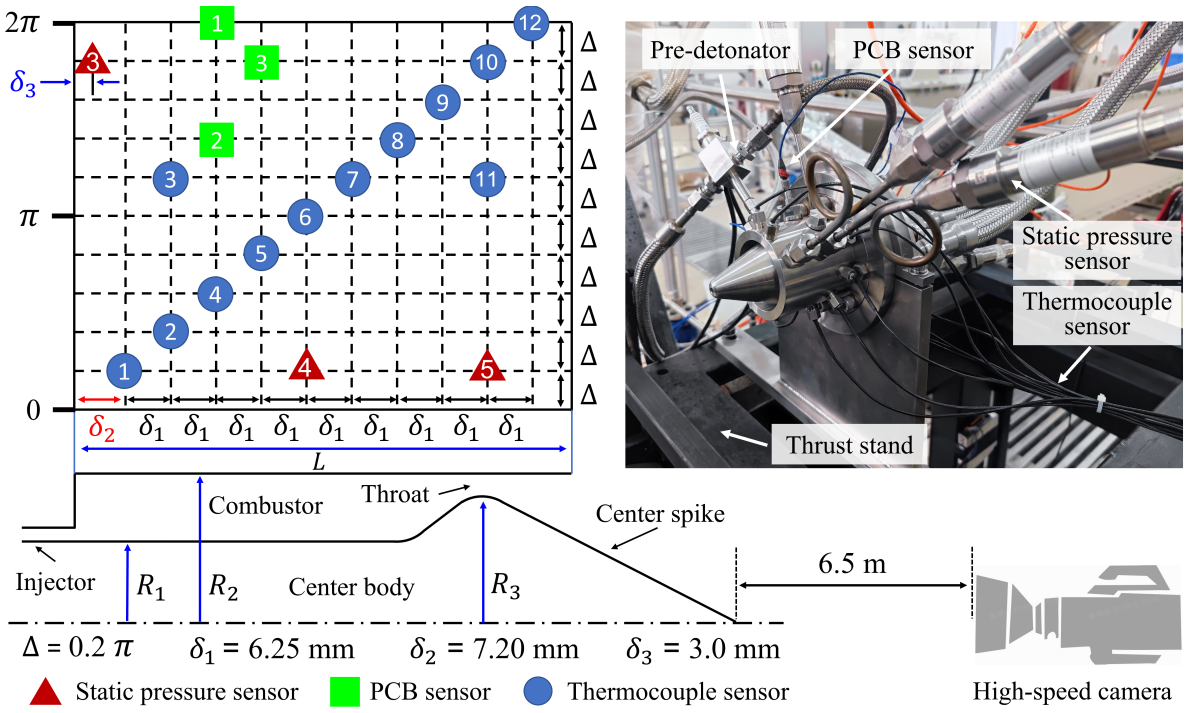

Figure 1: The experimental device, sensor arrangement and schematic diagram of RDC.

3 Results and discussion

Experimental results show that stable detonations were successfully formed in all tests. The contraction of the exhaust plume to the inner cone revealed that the outlet pressure is lower than the back pressure,

as shown in Fig. 2 (right). The interaction between the intercepting shock and the inner cone induces a reflected shock, and the shear layer is clearly visible.

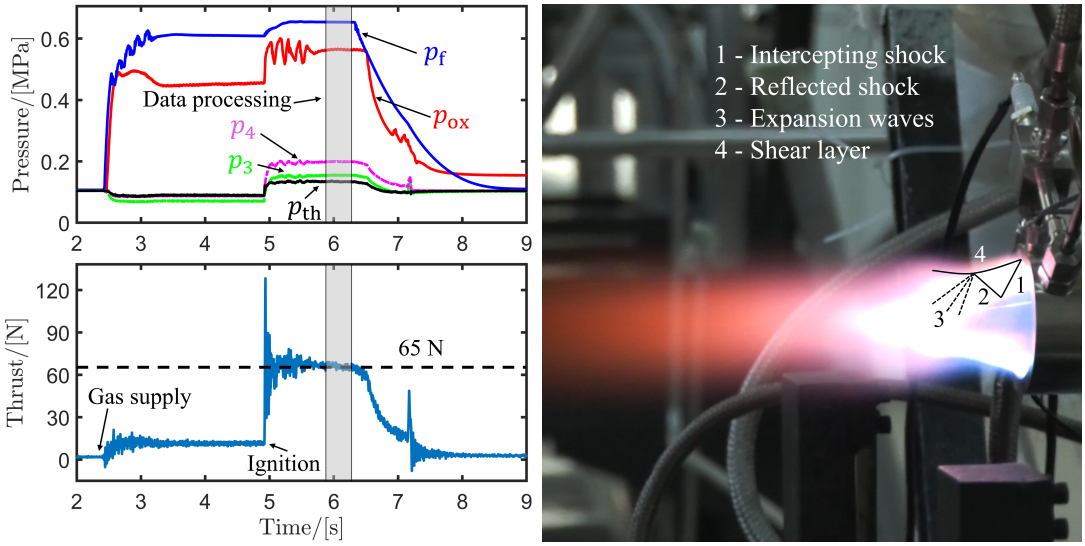

Figure 2: Criterion of experimental data selection, taking testas an example (left);The RDE exhaust plume during operation of test 3 (right).

Heat flux was determined based on temperature measurements using the Cook-Felderman technique. Assuming that heat is conducted into a semi-infinite body of known thermal properties, measured hot gas side wall temperature can be used to calculate heat flux into the wall according to the following equation [10]:

$$\dot{q}_n(t) = \frac{2\sqrt{\rho c k}}{\sqrt{\pi}} \sum_{i=1}^{n} \frac{T(t_i) - T(t_{i-1})}{(t_n - t_i)^{1/2} + (t_n - t_{i-1})^{1/2}}$$

where $\dot{q}$ - heat flux, $\sqrt{\rho c k}$ - material (thermocouple) constant, t - time, T - temperature.

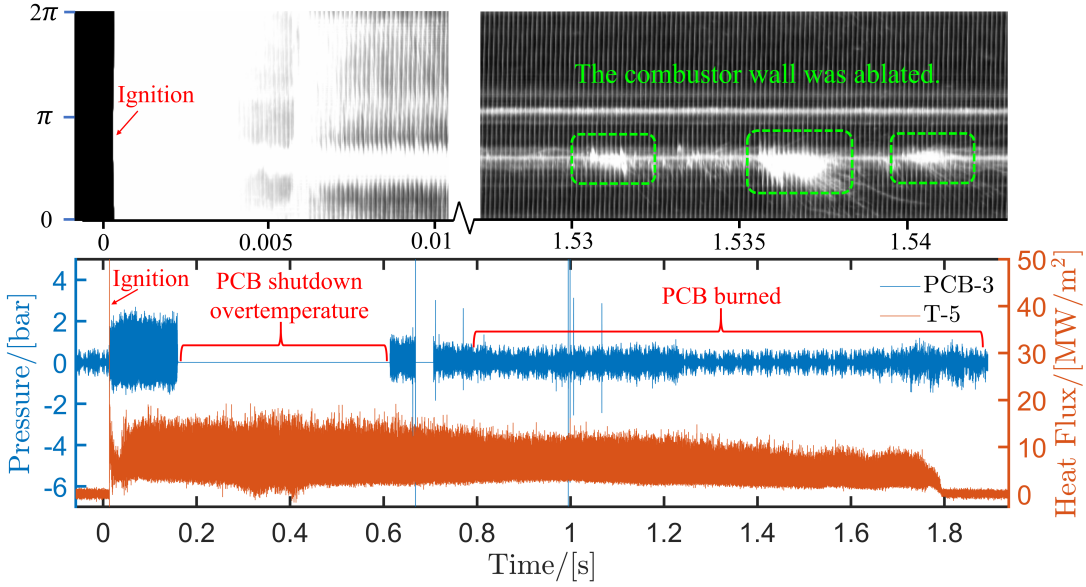

Figure 3: The space-time diagram, high-frequency pressure and heat flux curves of test 3. Mean thrust was 65 N, total mass flow was 72.7 g/s, and equivalence ratio (ER) was 0.93.

Figure 3 shows the space-time diagram, high-frequency pressure and heat flux curves of test 3. The space-time diagram shows that the engine has been in single-wave mode during operation and there is ablation on the inner wall of the combustor due to the high temperature environment. The RDW is further demonstrated by high frequency pressure curves and the PCB sensors only worked for about 150 ms before it burned out. The instantaneous heat flux in the combustor reaches 20 MW/m^2, indicating a high and transient heat load in the detonation region. It also shows that the thermocouple used can survive the whole experimental cycle, verifying its reliability and stability.

Figure 4 shows a comparison of the high-frequency heat flux and dynamic pressure curves of the detonation wave. Since the sampling rate of the PCB sensor is 5 times that of the thermocouple, the pressure curve is finer than the heat flux curve, and more data points are recorded. In other words, the heat flux curve obtained through the thermocouple has been filtered to some extent compared to the pressure curve. However, the transient variation of the heat flux is consistent with that of the pressure curve, indicating that the instantaneous heat flux is successfully captured by the thermocouple sensor. In particular, the phase difference between the heat flux peak and the pressure peak is half a wavelength, which coincides with the 180 degree difference between the two sensor positions in the circumferential direction. Therefore, this type of thermocouple can replace the PCB sensor, not only greatly reducing the cost, but also completely recording the transient characteristics of the detonation wave in the experiment.

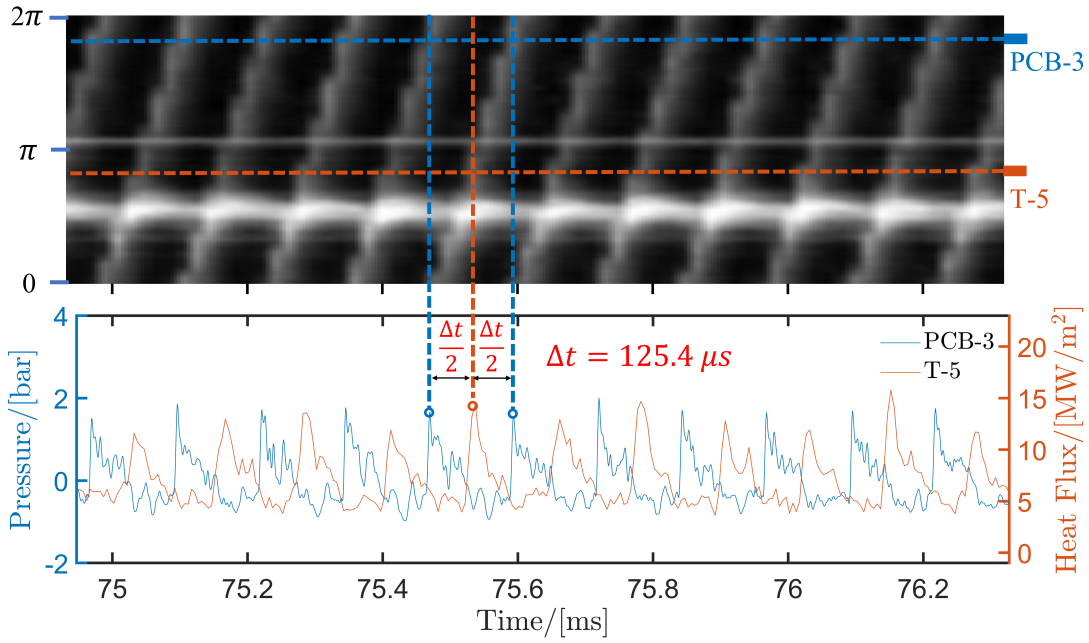

Figure 4: Comparison of the high-frequency pressure and heat flux curves of test 3.

The current experimental results show that the spatial distribution of the average heat flux has two high-point regions, namely the detonation region and the throat region, as shown in Fig. 5. Obviously, due to the existence of detonation wave, the average heat flux in the detonation wave region is the largest, reaching 9.6 MW/m^2. The reason for the increase of the average heat flux in the throat is that the mass flux reaches the maximum in this region. Therefore, the thermal protection and cooling design of these two regions need to be carefully considered, as the design of an effective cooling system is undoubtedly a key part of the engine development process. In addition, it is also found that with the increase of the equivalence ratio, the bulk heat flux presents a trend of first increasing and then decreasing. In the range of equivalence ratio 1.2-1.3, the bulk heat flux of the combustor basically reaches the maximum value. This may be related to the heat release rate of unit combustibles and the proportion of detonations. When

the equivalence ratio is relatively small, the combustor is dominated by detonations. As the proportion of combustibles increases, the heat release rate increases, which in turn increases the heat flux. But when the equivalence ratio is relatively large, a considerable proportion of the fuel is consumed by deflagration, which affects the intensity of the detonation wave, resulting in a decrease in heat flux.

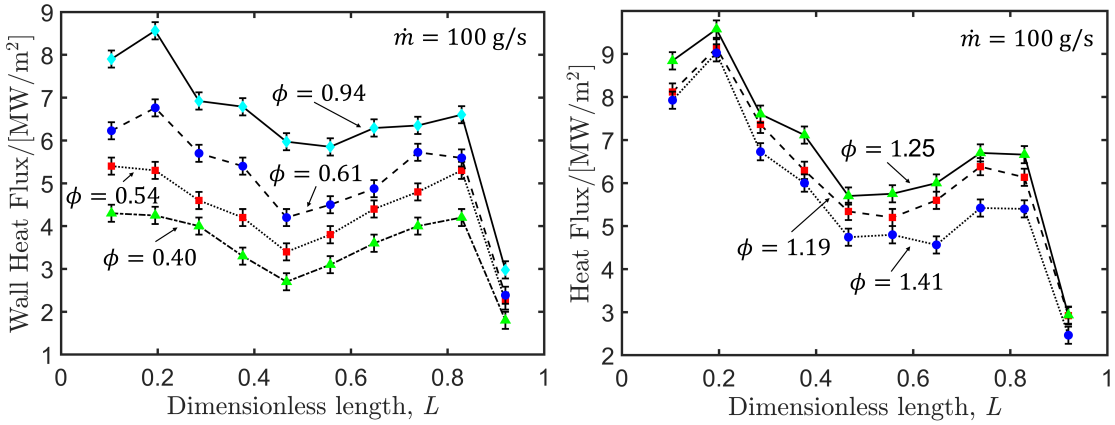

Figure 5: The spatial distribution of the average heat flux with different equivalence ratios at 100 g/s.

In addition, a weighted average of the heat fluxes in the head region of the combustor, where the positions of thermocouples No. 1 and No. 2 represent the detonation region, was made. The average heat flux in the detonation region is closely related to the equivalence ratio, as shown in Fig. 6 (left). Under the same mass flow rate, a trend of rising first and then falling was shown on the average heat flux with the increasing of equivalence ratio and the maximum value of average heat flux is in the range of equivalence ratio 1.2-1.3, which is consistent with the rule of the bulk heat flux of the combustor. Furthermore, it can be found that the average heat flux of the detonation region increases as the mass flow rate increases. Also, the bulk heat flux are closely related to the mass flow rate, as shown in Fig. 6 (right). Within the error range, the bulk heat flux increases with the increasing of the mass flow rate.

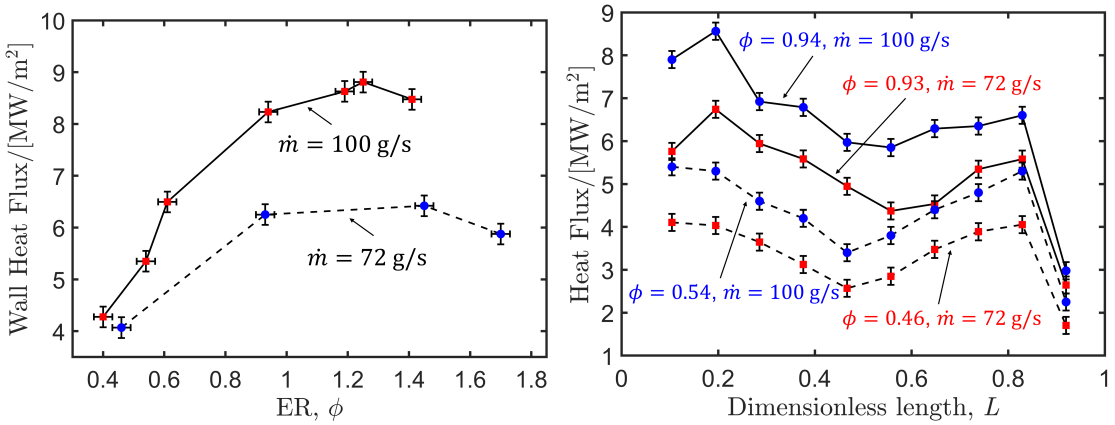

Figure 6: The average heat flux vs equivalence ratio in the detonation region (left); The spatial distribution of the average heat flux with different equivalence ratios and mass flow(right).

4 Conclusion

In order to evaluate the characteristics of instantaneous heat flux and the spatial distribution of the average heat flux, a compact RDE for space populsion was designed, and a series of effective experimental

tests were carried out using methane/GOX. The preliminary conclusions are as follows:

1. The instantaneous heat flux was successfully captured by the high-frequency thermocouple sensors, which is in good agreement with the peak of dynamic pressure. This type of thermocouple can be used as a substitute for the PCB sensor, which greatly reduces the cost and can obtain the characteristic signal of the detonation wave for a long duration.

2. The spatial distribution of the average heat flux has two high-point regions, namely the detonation region and the throat region. Thus the thermal protection and cooling design of these two areas need to be carefully considered.

3. Under the same mass flow rate, both the bulk heat flux and the average heat flux of the detonation area show a trend of rising first and then falling, and reach the maximum value in the range of equivalence ratio 1.2-1.3. And the bulk heat flux and the average heat flux of the detonation region increase with the increasing of the mass flow rate.

The above results are of great significance to the design of RDE cooling system.

References

[1] Ma J Z, Luan M Y, Xia Z J, et al. Recent Progress, Development Trends, and Consideration of Continuous Detonation Engines. AIAA Journal, 2020, 58(12):4976–5035.

[2] Nicholls J A, Wilkinson H R, Morrison R B. Intermittent detonation as a thrust-producing mechanism. Jet Propulsion, 1957, 27(5):534–541.

[3] Voitsekhovskii B V. Stationary Spin Detonation. Soviet Journal of Applied Mechanics and Technical Physics, 1960, (3):157–164.

[4] Meyer S J, Polanka M D, Schauer F, et al. Experimental Characterization of Heat Transfer Coefficients in a Rotating Detonation Engine. 55th AIAA Aerospace Sciences Meeting, Grapevine, Texas: American Institute of Aeronautics and Astronautics, 2017.

[5] Meyer S J, Polanka M D, Schauer F R, et al. Parameter Impact on Heat Flux in a Rotating Detonation Engine. 2018 AIAA Aerospace Sciences Meeting, Kissimmee, Florida: American Institute of Aeronautics and Astronautics, 2018.

[6] Kublik D, Kindracki J, Wolaski P. Evaluation of wall heat loads in the region of detonation propagation of detonative propulsion combustion chambers. Applied Thermal Engineering, 2019, 156:606–618.

[7] Lim D, Heister S D, Humble J, et al. Experimental Investigation of Wall Heat Flux in a Rotating Detonation Rocket Engine. Journal of Spacecraft and Rockets, 2021, 58(5):1444–1452.

[8] Goto K, Nishimura J, Kawasaki A, et al. Propulsive Performance and Heating Environment of Rotating Detonation Engine with Various Nozzles. Journal of Propulsion and Power, 2019, 35(1):213–223.

[9] Goto K, Ota K, Kawasaki A, et al. Cylindrical Rotating Detonation Engine with Propellant Injection Cooling. Journal of Propulsion and Power, 2022, 38(3):410–420.

[10] Schultz D, Jones T. Heat transfer measurements in short duration hypersonic facilities. Technical report, AGARD-AG-165, 1973.